J. Electroanal. Chem., 98 (1979) 171—180

THE PIEZOELECTRIC DETECTION OF ELECTRODE SURFACE PROCESSES

RICHARD E. MALPAS, RONALD A. FREDLEIN * and ALLEN J. BARD

Department of Chemistry, The University of Texas at Austin, Austin, Texas 78712 (U.S.A.)

(Received 2nd June 1978; in revised form 12th September 1978)

ABSTRACT

A technique is described for the observation of surface processes (e.g., adsorption, film formation) occurring on solid electrodes using a piezoelectric element to detect the derivative of the surface stress with potential. The technique is illustrated for the case of Pt in 1 *M* H_2SO_4, 1 *M* $HClO_4$ and 50 μM $AgNO_3$ in 1 *M* $HClO_4$. The formation and removal of oxide layers, adsorbed hydrogen and silver on Pt were observed to be in agreement with past electrochemical and optical studies. In addition, evidence for the occurrence of processes difficult to detect by electrochemical methods (e.g., oxide layer transformations) was obtained.

INTRODUCTION

An understanding of the solid electrode-solution interface and processes occurring on the electrode surface is fundamental to electrochemistry. The surface stress data on solid electrodes of Gokhshtein [1], Beck [2], Fredlein and Bockris [3], and Morcos [4] complement both electrochemical data [5,6] and the growing body of information from optical studies [7—12] which constitute the bulk of our knowledge of this interface. However, surface stress techniques on solids have received little attention because of their experimental difficulties. This paper reports an experimentally simple technique for obtaining interfacial information.

A piezoelectric material is one which develops a potential difference when subjected to a mechanical stress because of the generation of a net electrical dipole. Ceramic piezoelectric materials are inexpensive and commercially available and can develop very high voltages ($\sim 10^2$ V) for mm deflections. In the work described a ceramic piezoelectric disk is bonded to an electrode and changes in the piezoelectric signal with in situ scanning of the electrode potential are monitored. The technique is somewhat similar to that of Gokhshtein [13] but differs in the simplified electrode design, the use of commercial instrumentation and the use of low frequency alternating signals (230 Hz) which permits the observation of slower electrode processes.

* Permanent address: Department of Chemistry, University of Newcastle, N.S.W., Australia.

EXPERIMENTAL

A one compartment cell was used with a Pt wire counter electrode and either a saturated calomel (SCE) or a Ag/Ag^+ reference electrode. The working electrode was constructed by attaching 0.05 mm Pt foil to a PXE 5 piezoelectric ceramic disk (Ferroxcube Corporation, Saugerties, N.Y.) with epoxy cement (Devcon, 5-minute) as shown in Fig. 1. Care was taken to insure that the Pt electrode was insulated from the piezoelectric disk and the disk from the solution by the epoxy cement.

A block diagram of the apparatus is shown in Fig. 2. A PAR 173 potentiostat with a PAR 175 Universal programmer (Princeton Applied Research Corp.) was used to supply a linear potential ramp. A 230 Hz, 10 mV sinusoidal signal was superimposed from an oscillator (Wavetek VCG 114) or the internal oscillator of a PAR 5204 lock-in amplifier.

The signal from the piezoelectric disk was synchronously detected at the above frequency with the lock-in amplifier. The piezoelectric signal magnitude and phase angle were recorded simultaneously with the cyclic voltammogram

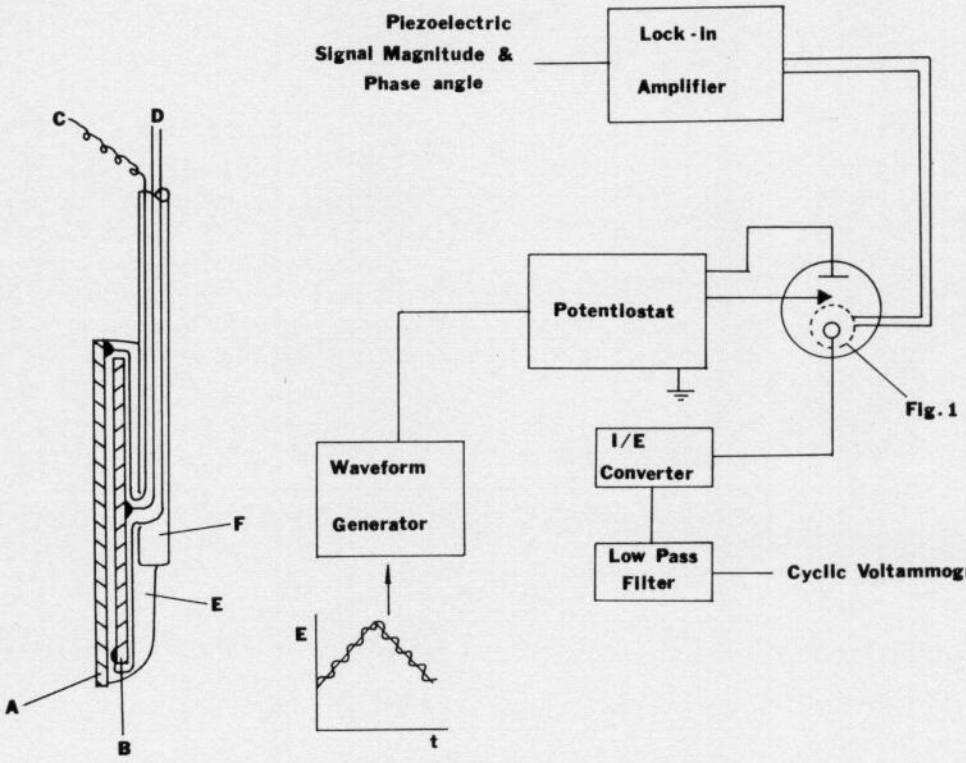

Fig. 1. The working electrode. (A) Pt foil (17 × 18 mm^2); (B) piezoelectric ceramic disk (ϕ = 16 mm; thickness = 0.2 mm); (C) lead to potentiostat; (d) leads to lock-in amplifier input; (E) epoxy cement; (F) pyrex glass tube.

Fig. 2. Block diagram of the apparatus.

(Houston Instruments 2000 XY recorders); alternately the in-phase and quadrature signals from the piezoelectric disk were recorded and the magnitude and phase angle calculated. No electromagnetic cross talk due to either capacitative or inductive coupling could be detected between the electrode and the piezoelectric disk. This was determined in a blank experiment in which an alternating current was imposed across the platinum electrode connected via a 100 Ω resistor to the counter electrode lead of the potentiostat, which generated currents through the Pt electrode of similar magnitudes as those found in the electrochemical experiments.

TREATMENT OF RESULTS

A step (or static) [14] stress on a piezoelectric disk generates a potential that decays through its own equivalent circuit (Fig. 3) [15,16] producing a potential pulse. The sign of this potential depends on the direction of the applied stress [17], so that an alternating stress produces an alternating potential. For the above electrode, changes in the electrode-solution interface, e.g. adsorption, film formation and double-layer rearrangement, accompanying a change of potential, result in a change of the surface stress, σ, of the electrode. The electrode and piezoelectric element are mechanically coupled and thus the applica-

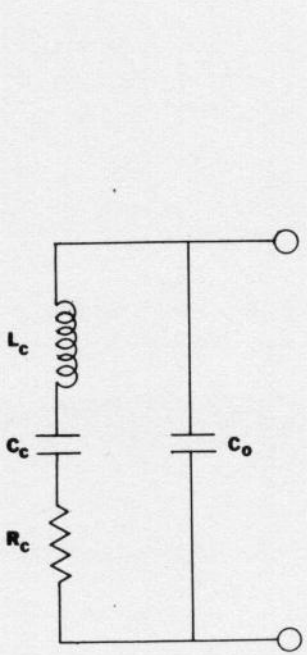

Fig. 3. The equivalent circuit of a piezoelectric disk. C_0 = the static capacitance of the disk; L_c, C_c, R_c = the equivalent inductance, capacitance and resistance of the disk.

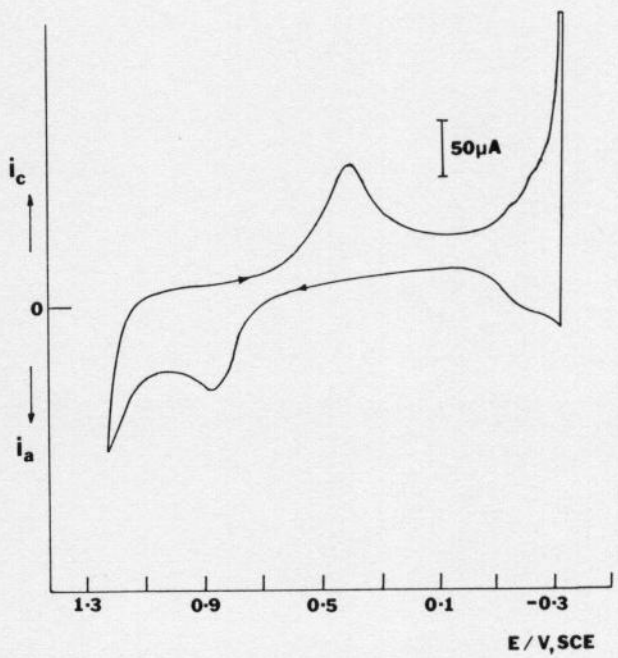

Fig. 4. Cyclic voltammogram for 1 M H_2SO_4 with a Pt electrode. Scan rate: 10 mV s^{-1}; electrode area: 3.1 cm^2.

tion of a small alternating signal, dE, to the electrode produces a piezoelectric output, the magnitude of which is proportional to $|d\sigma/dE|$. Changes in the sign of $d\sigma/dE$, caused by σ passing through an extremum, should be manifest by the magnitude decreasing to zero and a phase change of π. Numerical integration of the piezoelectric signal magnitude, taking into account the sign changes of $d\sigma/dE$ yield plots of a quantity Σ, which is linearly related to σ, against E. No attempt has been made in this study to determine the quantitative relationship between Σ and σ, which depends on the mechanical properties

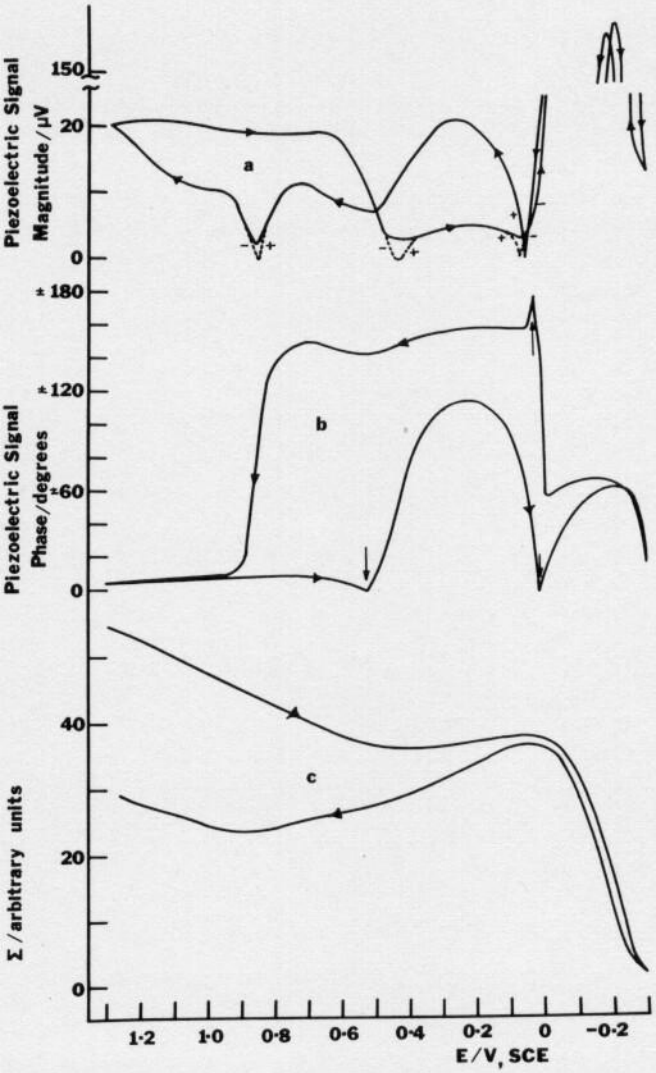

Fig. 5. Piezoelectric signals for 1 M H_2SO_4. (a) (Piezoelectric signal magnitude, E) plot. Dashed lines signify zero extrapolations (see text). (+, —) indicate the sign of the derivative (from ref. 18). (b) (Piezoelectric phase, E) plot. Arrows indicate phase angle sign changes. (c) (Σ, E) plot obtained by integration of (a).

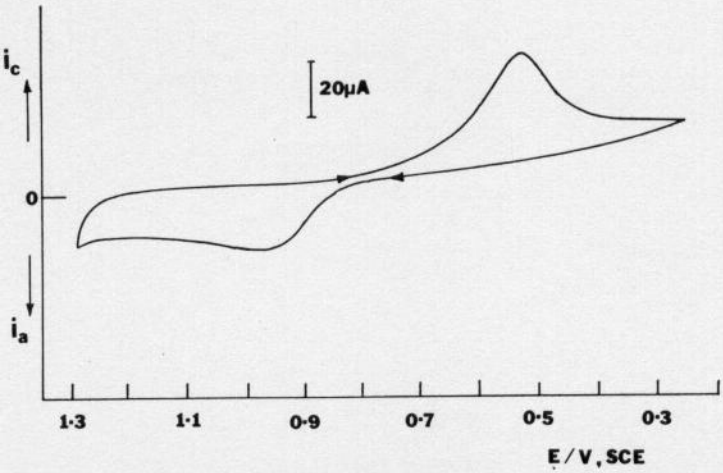

Fig. 6. Cyclic voltammograms for 1 *M* $HClO_4$ with a Pt electrode. Scan rate: 2 mV s^{-1}. Experimental technique as ref. 21.

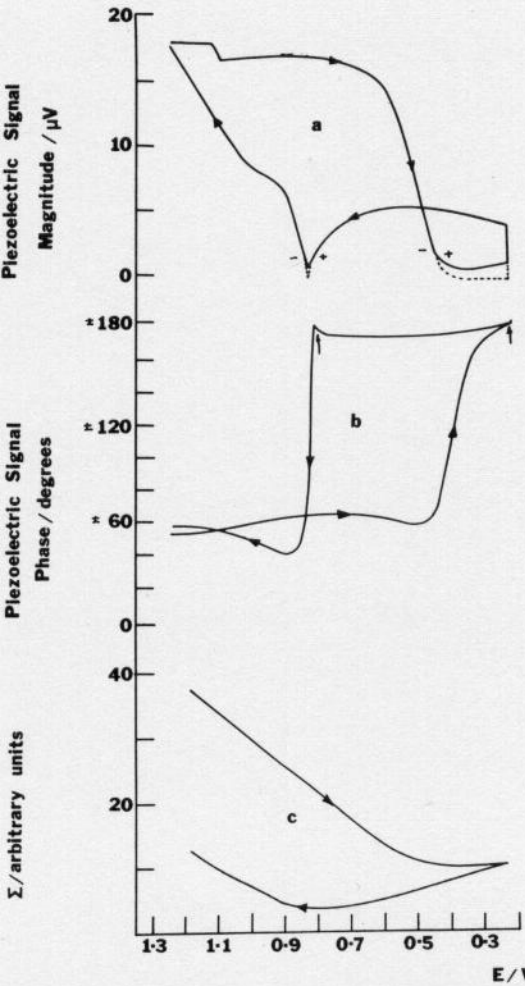

Fig. 7. (piezoelectric signals for 1 *M* $HClO_4$. Experimental technique as ref. 21. (a) Piezoelectric signal magnitude, *E*) plot. Dashed lines and (+, —) as for Fig. 5. (b) (Piezoelectric phase, *E*) plot. Arrows as for Fig. 5. (c) (Σ, *E*) plot obtained by integration of (a).

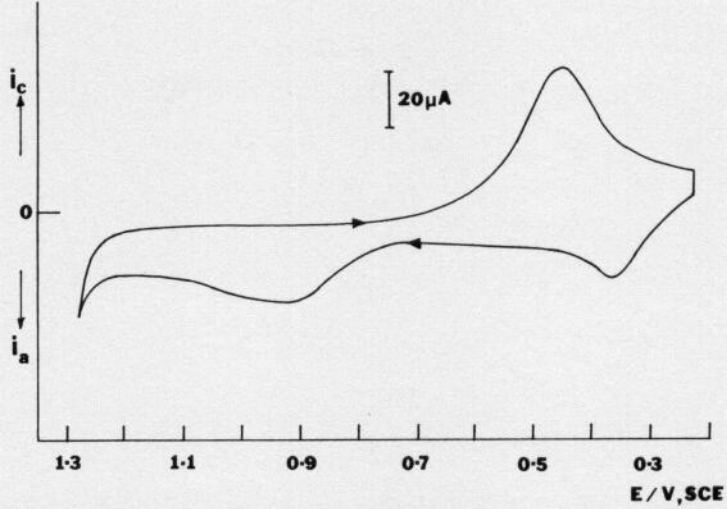

Fig. 8. Cyclic voltammogram for 50 μM $AgNO_3$ in 1 M $HClO_4$ with a Pt electrode. Scan rate: 2 mV s^{-1}. Experimental technique as ref. 21.

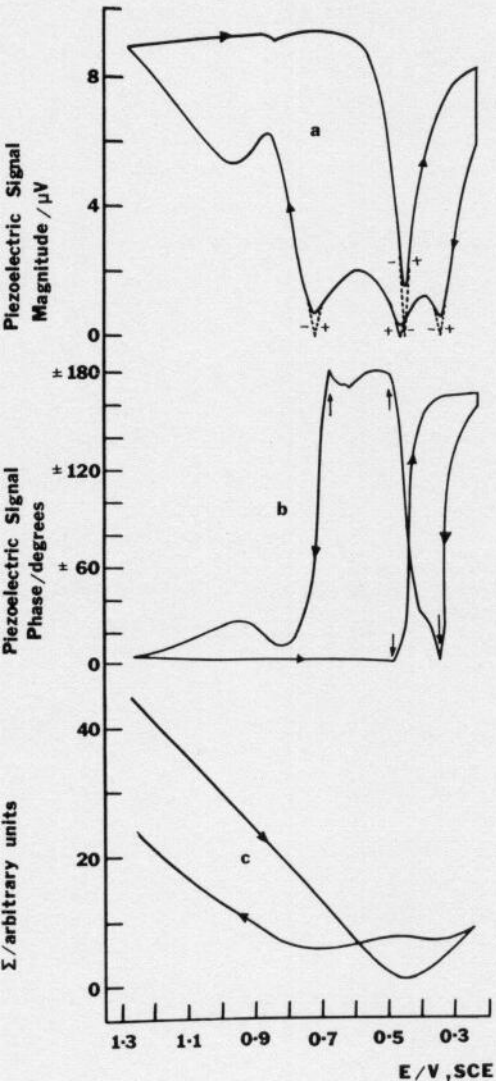

Fig. 9. Piezoelectric signals for 50 μM $AgNO_3$ in 1 M $HClO_4$. Experimental technique as ref. 21. (a) (Piezoelectric signal magnitude, E) plot. Dashed lines and (+, —) as for Fig. 5. (b) (Piezoelectric phase, E) plot. Arrows as for Fig. 5. (c) (Σ, E) plot obtained by integration of (a).

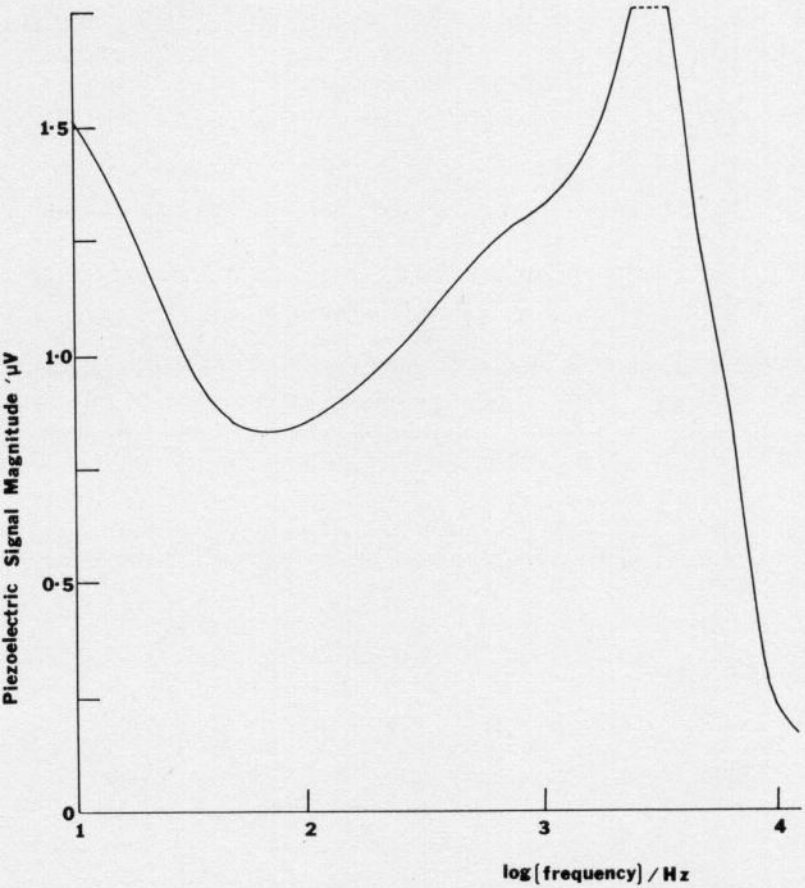

Fig. 10. Variation of piezoelectric magnitude with frequency of the applied alternating signal for 1 *M* H_2SO_4 at +0.3 V.

of the electrode system and the piezoelectric voltage response, but Σ is still a valuable aid to the interpretation of the data.

Results expressed in this way are shown for 1 *M* H_2SO_4 (Figs. 4 and 5), 1 *M* $HClO_4$ (Figs. 6 and 7) and 50 μM $AgNO_3$ in 1 *M* $HClO_4$ (Figs. 8 and 9). Integration of these systems was carried out by identifying the extremum at +0.05 V for the Pt-H_2SO_4 system as a maximum by comparison with the data of Fredlein et al. [18] for the same system. The non-zero magnitude minima and less than 180° phase changes observed in these systems at the positions of sign change (Figs. 5a, 7a, 9a) are probably due to the finite (10 mV) aplitude of the applied alternating signal, cf. Gokhshtein [19]. For integration these minima were extrapolated to zero.

The variation of the piezoelectric signal magnitude with applied alternating potential frequency, for the double-layer region of Pt-H_2SO_4, is shown in Fig. 10. Single resonance (~2 kHz) and antiresonance (~70 Hz) frequencies are consistent with the equivalent circuit of the piezoelectric disk (Fig. 3) and indicate that only one flexure mode (probably convexial) is important [15]. At low

operating frequencies (<50 Hz) the piezoelectric signal was very noisy, whereas high frequencies (>1 kHz) prevented the monitoring of slow interfacial processes; 230 Hz was chosen as a convenient compromise.

DISCUSSION

The piezoelectric signal magnitude was typically 10—100 μV at these scan rates (2—10 mV s^{-1}). This seems small considering the response to flexure (of the order of 250 V mm^{-1}) expected for the PXE 5 piezoelectric element, and may reflect source loading by the lock-in amplifier and poor mechanical coupling between the Pt foil and piezoelectric element. The (Σ, E) plot for H_2SO_4 (Fig. 5c) shows that on scanning in a negative direction from +1.3 V, a decrease in Σ with potential is observes to a minimum at +0.45 V. This corresponds to the reduction peak of the platinum oxide surface shown in the cyclic voltammogram (Fig. 4). As the scan continues in a negative direction the signal passes through a maximum at ~+0.05 V, in agreement with previous studies [18], corresponding to the onset of hydrogen adsorption. The sharp decrease in Σ following this maximum is probably caused by a change in the interfacial stress accompanying this process. On scan reversal the maximum corresponds to the completion of hydrogen desorption. The rise after the following minimum corresponds to the oxidation of the platinum surface as seen in the cyclic voltammogram and may possibly be caused by stressing of the electrode on formation of the oxide film. Hysteresis was observed between forward and reverse scans in previous steady-state measurements and is interpreted as being due to irreversible oxide formation [18]. The application of more positive potentials and the non steady-state technique could explain the increased hysteresis observed here.

It is possible that stresses generated by temperature changes at the electrode surface could also be detected. To test this possibility, an electrode reaction where both oxidized and reduced forms are soluble was investigated. Addition of 10^{-2} M $K_3Fe(CN)_6$ (the electrochemical Peltier effect of which has been previously investigated [20]) to the H_2SO_4 system gave a piezoelectric response essentially identical to that of H_2SO_4 alone, despite the appearance of the characteristic Fe(III)/Fe(II) reduction and oxidation waves at +0.45 V on the cyclic voltammogram. This indicates no contribution to σ from the enthalpy of the redox process at these concentrations.

The (Σ, E) plot for $HClO_4$ (Fig. 7c) is similar to H_2SO_4. Addition of Ag^+ (Fig. 9c), however, sharpens the broad minimum at ~+0.4 V (cathodic scan), the minimum at +0.84 shifts to +0.73 V and a new minimum appears at +0.35 V (both anodic scans). The system has been studied and characterized previously by McIntyre and Kolb [21] using specular reflectance spectroscopy. Their results are summarized and compared to the above extrema, in Table 1. A good correlation between their data and interpretations and these extrema is shown.

For all three systems further important information can be abstracted from the unintegrated piezoelectric magnitude plots. "Non-zero" (i.e., no π phase shift) extrema indicate electrochemical processes whose occurrence is not readily apparent from the cyclic voltammogram. For example, the maximum-minimum centered at ~0.9 V (anodic scan) for the $Ag^+/HClO_4$ system (Fig. 9a).

TABLE 1

Comparison of piezoelectric, electrochemical and reflectance data for Ag^+ in $HClO_4$

E [a,b]/V	E [c]/V	E [d]/V	Process [e]
Cathodic scan			
0.48 [f]	0.76 [g]	~0.45	Reduction of O layer and underpotential Ag deposition
Anodic scan			
0.36	0.31	0.35	Anodic dissolution of bulk Ag
0.91	0.66	0.73	Oxidative desorption of Ag monolayer and metal oxide formation

[a] All potentials V(SCE).
[b] From cyclic voltammogram (ref. 21).
[c] From reflectance measurements (ref. 21).
[d] Σ extrema.
[e] From ref. 19.
[f] O reduction peak potential.
[g] Commencement of O layer reduction.

Shoulders are also present for $HClO_4$ and H_2SO_4 (Figs. 5a) and 7a) at this potential, which is in close agreement with the potential at which Horkans et al. [11] observe a discontinuity in their ellipsometric data. This is interpreted as being caused by a change in the form of the oxide layer from Pt-OH to Pt-O at this potential.

The potentials of initial appearance and disappearance of surface films on the electrode can also be determined from the unintegrated plots. Thus, for $HClO_4$ (Fig. 7a) on the cathodic scan, the slope of the derivative starts to change at ~0.8 V corresponding to onset of oxide reduction, in agreement with optical data [11,12].

This technique can thus provide electrochemical information not readily obtainable from purely electrochemical studies. The electrode construction and instrumentation involved is simple and with further development of the technique could yield information, complementary to optical data, on a wide number of electrochemical systems.

ACKNOWLEDGMENTS

The authors would like to thank Ferroxcube Corp. for supplying the piezoelectric ceramic disks. Financial support by the Robert A. Welch Foundation and the National Science Foundation is gratefully acknowledged.

REFERENCES

1 A.Ya. Gokhshtein, Russian Chem. Rev., 44 (1975) 921.
2 T.R. Beck, J. Phys. Chem., 73 (1969) 446; K.F. Lin and T.R. Beck, J. Electrochem. Soc., 123 (1976) 1145.
3 R.A. Fredlein and J.O'M. Bockris, Surface Sci., 46 (1974) 641.
4 I. Morcos, J. Electroanal. Chem., 62 (1975) 313.

5 R. Woods in A.J. Bard (Ed.), Electroanalytical Chemistry, Vol. 9, Marcel Dekker, New York, 1976.
6 B.E. Conway, H. Angerstein-Kozlowska and F.C. Ho, J. Vac. Sci. Technol., 14 (1977) 351.
7 Optical Techniques in Electrochemistry in R.H. Muller (Ed.), Advances in Electrochemistry and Electrochemical Engineering, Vol. 9, Wiley-Interscience, New York, 1973.
8 W.R. Hinemann, Anal. Chem., 50 (1978) 390A.
9 A.J. McQuillan, P.J. Hendra and M. Fleishmann, J. Electroanal. Chem., 65 (1975) 933.
10 R.P. Cooney, M. Fleishmann and P.J. Hendra, J. Chem. Soc. Chem. Commun., (1977) 235.
11 J. Horkans, B.D. Cahan and E. Yeager, Surface Sci., 46 (1974) 1.
12 W.E. O'Grady, M.Y.C. Wo, P.L. Hagans and E. Yeager, J. Vac. Sci. Technol., 14 (1977) 365.
13 A. Ya. Gokhshtein, Sov. Electrochem., 2 (1966) 1318.
14 W.G. Cady, Piezoelectricity, McGraw-Hill, New York, 1946.
15 R. Kazys and E. Mazak, Acustica, 28 (1973) 208.
16 B. Ramadan and J.F. Kos, Rev. Sci. Instrum., 49 (1978) 374.
17 J. Van Randeraat and R.E. Setterington (Eds.), Piezoelectric Ceramics, N.V. Philips, Eindhoven, The Netherlands, 1974.
18 R.A. Fredlein, A. Damjanovic and J.O'M. Bockris, Surface Sci., 25 (1971) 261.
19 A.Ya. Gokhshtein, Sov. Electrochem., 4 (1968) 590.
20 R. Ramamushi, J. Electroanal. Chem., 65 (1975) 263.